FREQUENCY-INDEPENDENT BEAMFORMER WITH LOW RESPONSE ERROR

Thomas Chou

Massachusetts Institute of Technology, Cambridge, MA
and
AT&T Bell Laboratories, Murray Hill, NJ

ABSTRACT

A method is developed for designing broadband beamformers with highly frequency-invariant behavior. The method combines harmonic nesting with filter-and-sum beamforming, yielding systems with efficient log-periodic transducer structures and plane wave responses which deviate from the desired response by less than 1% of the peak mainlobe response. In particular, null locations are very constant with frequency, allowing the nulling of directional broadband interference. A digital implementation covering audio frequencies (500 - 7200 Hz) is built and demonstrates results in good agreement with simulations, yielding deviations under 5% of peak response.

1. OVERVIEW

The use of transducer arrays for spatial filtering of propagating waves is well established. Applications include sonar, radio, radar, acoustic imaging, and teleconferencing equipment. Many applications involve broadband signals such as speech, music, and spread-spectrum signals. Arrays for such broadband signals are often difficult to design since array properties can be highly frequency-dependent. In particular, frequency-dependent lobe widths cause some signals to be received with distorted spectra. Also, frequency-dependent null locations impair the ability to cancel broadband interference.

Figure 1 shows the directivity patterns of a simple eleven-element array with uniform weighting and uniform element spacing. Evidently, the directivity pattern contracts in proportion to increasing frequency, causing variations in both mainlobe shape and sidelobe/null locations.

A number of so-called *constant-beamwidth* solutions address mainlobe width variations but still have significant variations in sidelobe and in null behavior [1, 2, 4, 5].

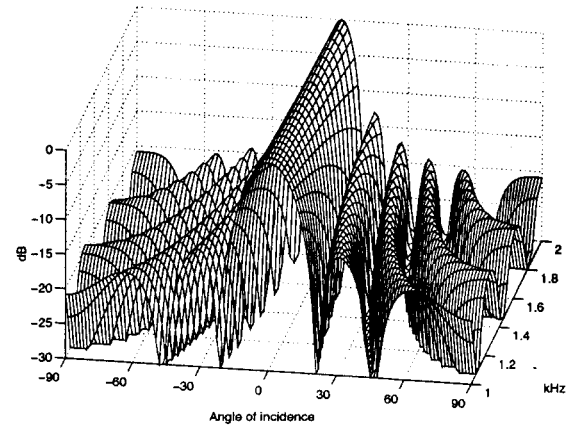

Figure 1: Plane wave response of simple delay-and-sum beamformer. Angle of incidence is measured relative to broadside in this and all other figures.

The solution presented here combines the ideas of harmonic nesting and filter-and-sum beamforming to correct both types of variations over arbitrarily large frequency ranges:

2. HARMONIC NESTING

The harmonic nesting approach is to cover a large frequency range by implementing several subarrays, each designed for a smaller frequency range, typically an octave. The subarrays are physically superimposed, and their outputs are electronically summed. This log-periodic structure is more economical than a single uniformly spaced array, since element count is logarithmically rather than linearly related to ratio of highest to lowest operating frequencies.

Figure 2 shows the transducer geometry used in the four-octave beamformer implemented in this work. Note the additional economization in that some ele-

0-7803-2431-5/95 $4.00

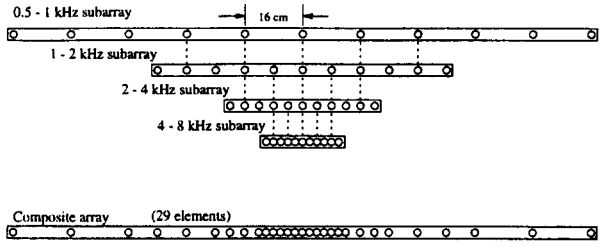

Figure 2: Transducer configuration of four-octave nested array. Dotted vertical lines represent elements which are common to more than one subarray.

ments are shared among subarrays.

2.1. Filter-and-sum beamforming

The harmonic nesting just described reduces a broadband beamforming problem to a set of octave beamforming problems. The frequency-variations within the octave are then controlled by the frequency-dependent element weights implemented by a *filter-and-sum* beamformer structure, as shown in Figure 3. The array response to a plane wave having frequency ω and incidence angle θ (measured relative to broadside) is:

$$O(\theta,\omega) = B(\omega) \sum_{n=-N}^{N} e^{j\frac{\omega}{c_s} dn \sin\theta} H_n(\omega), \qquad (1)$$

where c_s is the velocity of sound, $H_n(\omega)$ is the frequency response of the nth elemental filter, and $B(\omega)$ is the frequency response of the bandpass filter, if it exists. Note the Fourier-like appearance of this expression, which is exploited in step 2 of the following procedure for designing the array and filters of the filter-and-sum structure.

1. Determine the microphone geometry. Inter-element spacing must be at most $c_s/(4f_0)$ to avoid aliasing. The array span L is typically determined by selectivity requirements, in that mainlobe width is approximately proportional to $f/(Lc_s)$.

2. Select the desired array pattern $R(u)$, where $u = k_x c/\omega$ which for ordinary propagating waves equals $\sin\theta$, θ being the incidence angle of the incoming waves.

3. Select a set of K frequency values $f_1, f_2, \ldots f_K$ such that $f_1 = f_0$, $f_K = 2f_0$, and the remaining values are uniformly distributed in the range $[f_0, 2f_0]$. Compute the element weights for each frequency value by taking an inverse discrete Fourier transform of the sampled desired pattern $R(u_n)$, where:

$$u_n = \frac{c\,n}{f_j dM}, \quad -N \le n \le N, \; 1 \le j \le K, \qquad (2)$$

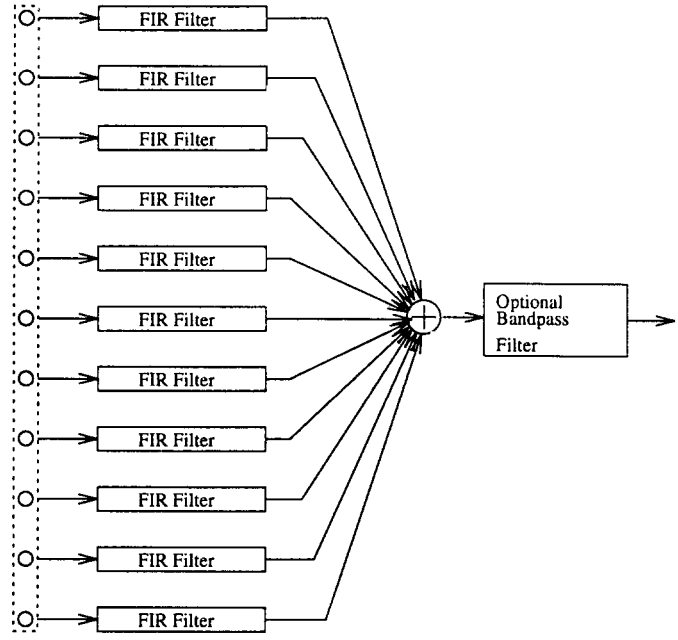

Figure 3: Filter-and-sum structure.

This process determines the desired frequency response of each elemental filter at K in-band frequency values. The desired response for out-of-band frequencies is assumed to be zero.

4. For each element, many well-known FIR filter design methods are available to design the elemental filter from the frequency response constraints determined in step 2.1. A frequency-sampling approach (such as that described in [3]) has been tried and gives good results.

This process can usefully be viewed as a 2-dimensional FIR filter design. To see this, define $\omega_x = k_x d$ and $\omega_y = \omega T$ and define a desired 2-D filter response which is related to the desired array pattern by:

$$X(\omega_x,\omega_y) = R(\frac{\omega_x T c_s}{\omega_y d}). \qquad (3)$$

(Note that $X(\omega_x,\omega_y)$ is the familiar wavenumber-frequency response scaled such that both frequency variables have dimensions of radians only.) The above steps design a set of M FIR filters, having coefficients that can be organized into a 2-D function having a 2-D Fourier transform exactly equal to $X(\omega_x,\omega_y)$ at the following rectangular grid of $K \times M$ points:

$$(\omega_x,\omega_y) = (\frac{2\pi n d}{M}, 2\pi f_j T), \quad -N \le n \le N, 1 \le j \le K. \qquad (4)$$

Clearly, there are interpolation errors due to the sampling operation. One method of reducing these errors is to increase the sampling density. The sampling

density in the ω_y dimension is related to the elemental FIR filter lengths, which can be made quite high with current digital signal processing hardware. However, the sampling density in the ω_x dimension depends on M, the number of array elements, which may be more subject to economic and physical constraints.

Reducing the interpolation error along the ω_x dimension can also be achieved via different filter design techniques, or by judicious selection of the desired array pattern $R(u)$. The latter is demonstrated in the following design example:

3. DESIGN EXAMPLE

The design steps are carried out for a 1 - 2 kHz beamformer having 11 elements:

1. Since $f_0 = 1000$, the inter-element spacing must be at most $\frac{343}{4f_0} = 8.57$ centimeters. A spacing of exactly 8 cm was used. The microphones chosen were first order gradients, having a dipole response proportional to $\cos\theta$.

2. One obvious choice for $R(u)$ is the Fourier transform of a continuous aperture having the same effective span as the discrete array, i.e. a sinc function:

$$R(u) = \frac{\sin(\frac{11}{4}\pi u)}{\frac{11}{4}\pi u} \tag{5}$$

This pattern cannot be exactly realized at any frequency. This deficiency is corrected in the following "periodic sinc":

$$R(u) = \frac{\sin(\frac{5}{2}\pi u)}{5\sin(\frac{1}{2}\pi u)}. \tag{6}$$

This function is exactly realizable at both f_0 and $2f_0$, and results in a plane wave response having a lower absolute difference from the desired response (0.005 versus 0.01 for the ordinary sinc, when the mainlobe response is normalized to unity). The tradeoff is a 10 percent wider mainlobe, as well as extra grating lobes in the invisible region which increase the sensitivity to uncorrelated noise.

In this application, the ordinary sinc was chosen over the periodic sinc because experimental errors are large (0.05) compared to the numerical errors.

3. The computations in the third step are carried out with $K = 6$.

4. The FIR filters are designed using a frequency-sampling approach, with a slight modification involving the frequency samples required by this algorithm. It was found that by reducing the sampling density in the out-of-band frequencies, the FIR filter lengths were lowered without significant performance degradation.

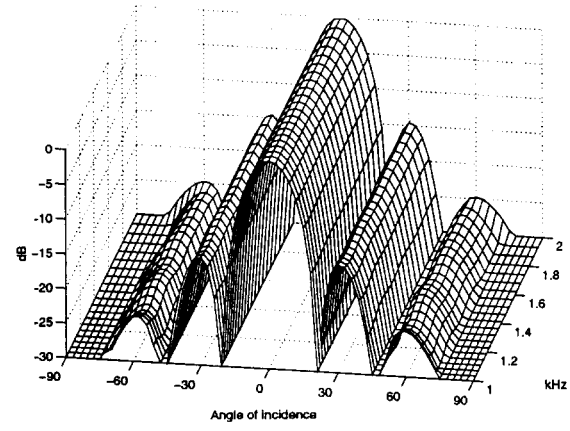

Figure 4: Response of filter-and-sum beamformer.

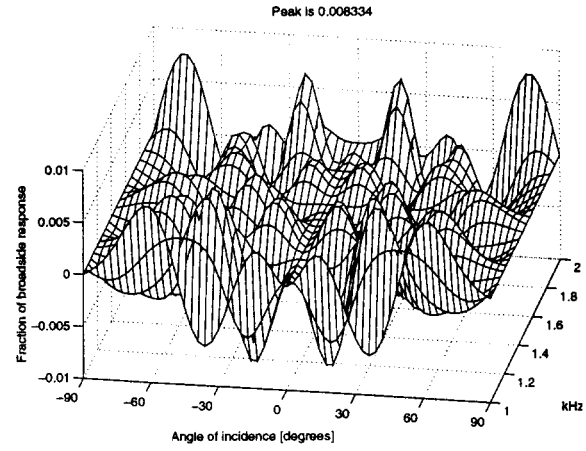

Figure 5: Simulated deviation from ideal frequency-independent response.

4. SIMULATED RESULTS

The design results were first evaluated using computer simulations of the actual beamforming hardware. Figure 4 shows the computed plane-wave response. Figure 5 shows the deviations between this response and that of a perfectly frequency-independent beamformer formed by averaging the simulated response over the octave. These deviations, which were computed with mainlobe responses normalized to unity, are quite low - never exceeding 0.01.

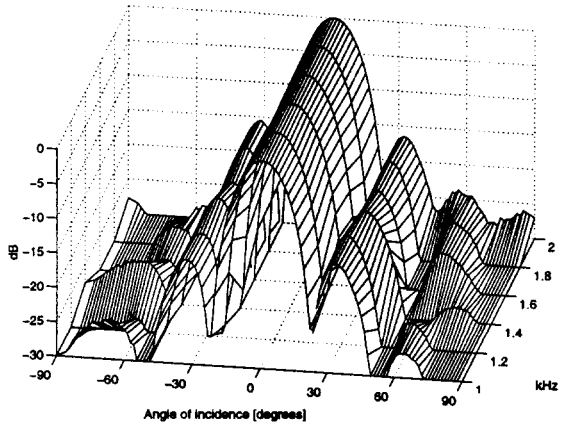

Figure 6: Experimentally determined response

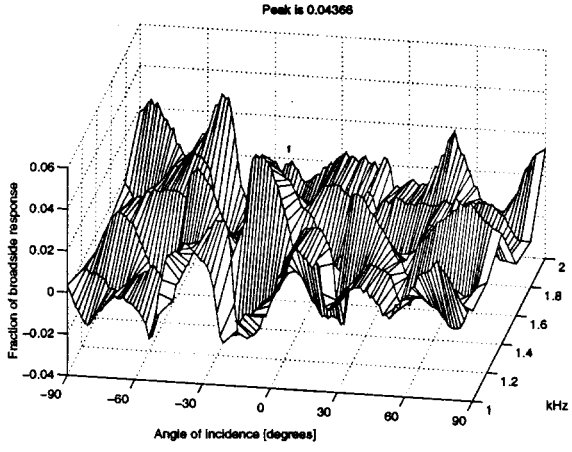

Figure 7: Deviation from ideal frequency-independent response

5. EXPERIMENTAL RESULTS

A real-time digital implementation was also developed. Figure 6 shows the plane-wave response as determined from anechoic chamber measurements. Figure 7 is obtained from Figure 6 in the same way Figure 5 is obtained from Figure 4. The peak error is still small, remaining under 5% of the peak mainlobe response.

A comparison of the overall simulated response with the overall measured response is also instrumental. This is shown in Figure 8. Again, agreement is good except for a slight broadening of measured beamshape, possibly due to imperfections in the physical hardware.

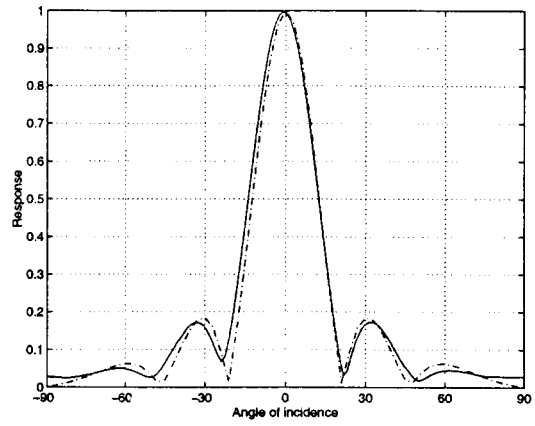

Figure 8: Comparison of simulated (dotted line) and experimental (solid line) responses.

6. CONCLUSIONS, EXTENSIONS

A beamformer design and implementation are shown to have highly frequency-independent behavior. Errors in plane wave response are under 1% and 5% of mainlobe response for computed and experimental behavior respectively. In particular, null locations are quite constant with frequency.

This approach can be made adaptive by computing a set of orthogonal pre-formed beams, leading to a *partially adaptive* structure with an attractively low number of adaptive parameters.

7. REFERENCES

[1] Michael M. Goodwin and Gary W. Elko. Constant beamwidth beamforming. *International Conference on Acoustics, Speech, and Signal Processing*, pages 169–172, 1993.

[2] E. L. Hixson and K. T. Au. Wide-bandwidth constant beamwidth acoustic array. *Journal of the Acoustical Society of America*, 48(1):117, July 1970.

[3] L. R. Rabiner and Bernard Gold. *Theory and Application of Digital Signal Processing.* Prentice-Hall, Inc., 1975.

[4] R. P. Smith. Constant beamwidth receiving arrays for broad band sonar systems. *Acustica*, 23:21–26, 1970.

[5] D. G. Tucker. Arrays with constant beam-width over a wide frequency-range. *Nature*, 180:496–7, September 1957.